An Innovative Sparseness-Promoting Inverse Scattering Approach Based on the Born Iterative Method

G. Oliveri, L. Poli, N. Anselmi, M. Salucci, and A. Massa

Abstract

In this work, non-Born targets are imaged through a novel inverse scattering (*IS*) methodology in microwave regime. The proposed method is based on a sparseness-promoting approach formulated within the single-task Bayesian compressive sensing (*ST-BCS*) framework. Moreover, the *ST-BCS* solver is effectively combined with a Born iterative method (*BIM*) inversion strategy to retrieve the target contrast while estimating the total electric field inside the imaged domain without recurring to time-consuming full-wave simulations. Some preliminary numerical results are reported to assess the effectiveness of the proposed *BIM-ST-BCS* method, as well as to highlight its current limitations.

Contents

Legenda

BCS: Bayesian Compressive Sensing

$ST-BCS$: Standard Bayesian Compressive Sensing

$MT-BCS$: Multi Task Bayesian Compressive Sensing

MoM: Method of Moments

BA : First Born approximation

BIM : Born Iterative Method

MSE : Mean Squared Error

CG : Conjugate Gradient

CSI : Contrast Source Inversion

1 Mathematical Formulation

Let us consider an inaccessible investigation domain Λ irradiated by a set of incident transverse-magnetic planes $E^v_{inc}(\mathbf{r}^v)$, $v = 1, ..., V$, impinging from the angular directions $\theta^v = \frac{2\pi}{V}(v-1)$, being V the number of views. In this working scenario, the scattered field $E^v_{scatt}(\mathbf{r}^v_s)$, $s = 1, ..., S$, is supposed to be measured through a set of S sensors equally displaced on a circular observation domain Θ, external to the investigation domain ($\Lambda \cap \Theta = 0$), having radius ρ. The exact location of the sensors are identified by the position vector $\mathbf{r}^v_s = (\rho\cos\theta^v_s \sin\theta^v_s)$, being $\theta^v_s = \theta^v + \frac{2\pi}{S}(s-1)$. This scattered field is known to be dependent on the equivalent currents $J^v_{eq}(\mathbf{r})$ generated in the support of the unknown scatterers placed into the domain Λ, according to the *data equation:*

$$E^v_{scatt}(\mathbf{r}^v_s) = -k_0^2 \int_\Lambda J^v_{eq}(\mathbf{r}') G(\mathbf{r}^v_s/\mathbf{r}')\, d\mathbf{r}' \tag{1}$$

where $G(\mathbf{r}^v_s/\mathbf{r}')$ is the Green's function in the free space and $k_0 = \omega\sqrt{\varepsilon_0\mu_0}$. The material properties of the investigation domain Λ in terms of relative dielectric permittivity $\varepsilon_r(\mathbf{r})$ and electric conductivity $\sigma(\mathbf{r})$ are described by means of the object function $\tau(\mathbf{r}) = \varepsilon_r(\mathbf{r}) - \varepsilon_0 - \frac{\sigma(\mathbf{r})}{2\pi f \varepsilon_0}$, being f the frequency of the TM plane wave.

In order to solve the problem, we have to discretise the *data equation,* so we have decided to use the MoM point matching version with a pixel-based approch. The investigation domain it is divided in N subdomains, in which our unknown $J^v_{eq}(\mathbf{r})$ it is considered constant. The basis functions have this form:

$$q_n(\mathbf{r}) = \begin{cases} +1 & \mathbf{r} \in D_n \\ 0 & \mathbf{r} \notin D_n \end{cases} \tag{2}$$

where D_n is the n-th subdomain (pixel). Instead the testing functions are Dirac δ:

$$\psi(\mathbf{r}) = \delta(\mathbf{r} - \mathbf{r}') \tag{3}$$

Now we can rewrite the *data equation* as follows:

$$[E^v_{scatt}] = [G^{ext}][J^v_{eq}] \tag{4}$$

where $[G^{ext}]$ is the external Green's function that links the position vector in the observation domain with those in the investigation domain.

The equivalent current $J_{eq}^{v}(\mathbf{r})$ depends on two unknown variables:

- the object function $\tau(\mathbf{r})$;
- the total electric field in the investigation domain $E_{tot}^{int}(\mathbf{r})$.

So our problem is Bilinear. Using the First Born Approximation we can make it linear. In this case, $E_{tot}^{int}(\mathbf{r})$ is considered equal to $E_{inc}^{v}(\mathbf{r})$ (known quantity). But this approximation can be apply only under the hypothesis of weak scatterators. The *data equation* is now:

$$[E_{scatt}^{v}] = [G^{ext}][E_{inc}^{v}][\tau] \tag{5}$$

To mitigate ill-posedness and ill-conditioning, which affects inverse scattering, regularization approches have been adopted thanks to their capability to effectively exploit a-priori information avaiable on the unknown scatterers. Within this line of reasoning, several probababilistic sparsity regularized formulations have been recently adopted in microwave imaging through the riformulation of the associated inverse problem in terms of suitable linear Bayesian Compressive Sensing (BCS) ones. This approch is now restricted to the condition of weak scattereres because of the Born approximation. In order to overcome this issues, we want to develop a novel method in the BCS framework that iteractively recostruct the dielectric features of the scatterers by progressively updating the total electric field (initially forced equal to the incident electric field) on the basis of the information acquired at the previous step.

FIRST ITERATION:

$$E_{tot}^{int}(\mathbf{r}) = E_{inc}(\mathbf{r}) \tag{6}$$

from the *data equation:*

$$[E_{scatt}] = [G^{ext}][E_{inc}][\tau] \tag{7}$$

SECOND ITERATION:

we can use the information acquired at the previous iteration:

$$\begin{cases} [E_{tot}^{int}] = [E_{scatt}^{int}] + [E_{inc}] \\ [E_{scatt}^{int}] = [G^{int}][E_{inc}][\tau] \end{cases} \tag{8}$$

now in the *data equation* we can put the new value of $[E_{tot}^{int}]$ and we recalculate the $[E_{scatt}]$:

$$[E_{scatt}] = [G^{ext}][E_{tot}^{int}][\tau] \tag{9}$$

i-th ITERATION:

we can use the information acquired at the $(i-1)$-th iteration. For this reason we define:

- $[E_{tot}^{int}]_i$ =the new value of $[E_{tot}^{int}]$ for the i-th iteration
- $[E_{scatt}^{int}]_{i-1}$ =$[E_{scatt}^{int}]$ generated by the reconstructed object at the $(i-1)$-th iteration
- $[\tau]_{i-1}$ =object function evalueted at the $(i-1)$-th iteration
- $[\tau]_i$ =object fanction evalueted at the i-th iteration

We update the $[E_{tot}^{int}]$ with the following system:

$$\begin{cases} [E_{tot}^{int}]_i = [E_{scatt}^{int}]_{i-1} + [E_{inc}] \\ [E_{scatt}^{int}]_{i-1} = [G^{int}][E_{tot}^{int}]_{i-1}[\tau]_{i-1} \end{cases} \tag{10}$$

we repeat those steps until we reach a certain threshold η or maxime number of iterations (I_{MAX}).

For the threshold we have considered the MSE of the relative dielectric permittivity(ε_r) reconstructed in two following iterations. To estimate the MSE we have used this formula:

$$MSE = \frac{1}{N}\sum_{n=1}^{N}[\varepsilon_r^i(n) - \varepsilon_r^{i-1}(n)]^2 \tag{11}$$

where:

- n =number of cells in which the investigation domain is divided
- $\varepsilon_r^i(n)$, $n = 1, ..., N$ =relative dielectric permittivity of the i-th iteration
- $\varepsilon_r^{i-1}(n)$, $n = 1, ..., N$ =relative dielectric permittivity of the $i-1$-th iteration

If $MSE < \eta$, the Born Iterative Method will stop.

2 Preliminary Numerical Assessment

2.1 Rectangle-shaped Object, $\ell = \lambda/6$, $h = \lambda/3$

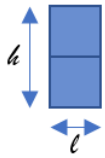

Figure 1: Rectangle-shaped Object

Test Case Description

Direct solver:

- Cubic domain divided in $\sqrt{D} \times \sqrt{D}$ cells
- Number of cells for the direct solver: $D = 1296$ (discretization $= \lambda/12$)

Inverse solver:

- Cubic domain divided in $\sqrt{N} \times \sqrt{N}$ cells
- Number of cells for the inversion: $N = 324$ (discretization $= \lambda/6$)

Measurement domain:

- Total number of measurements: $M = 27$
- Measurement points placed on circles of radius $\rho = 3\lambda$

Sources:

- Plane waves
- Number of views: $V = 27$; $\theta_{inc}^{v} = 0^\circ + (v-1) \times (360/V)$
- Amplitude: $A = 1.0$
- Frequency: $F = 300$ MHz ($\lambda = 1$)

Background:

- $\varepsilon_r = 1.0$
- $\sigma = 0$ [S/m]

Scatterer

- Rectangle-shaped object, $\ell = \lambda/6$, $h = \lambda/3$
- $\varepsilon_r \in 4.0$
- $\sigma = 0$ [S/m]

Born Iterative Method

- $I_{MAX} = 10$
- $\eta = 10^{-3}$

2.1.1 Rectangle-shaped Object, $\ell = \lambda/6$, $h = \lambda/3$, - ST-BCS reconstructed profiles with first Born approximation

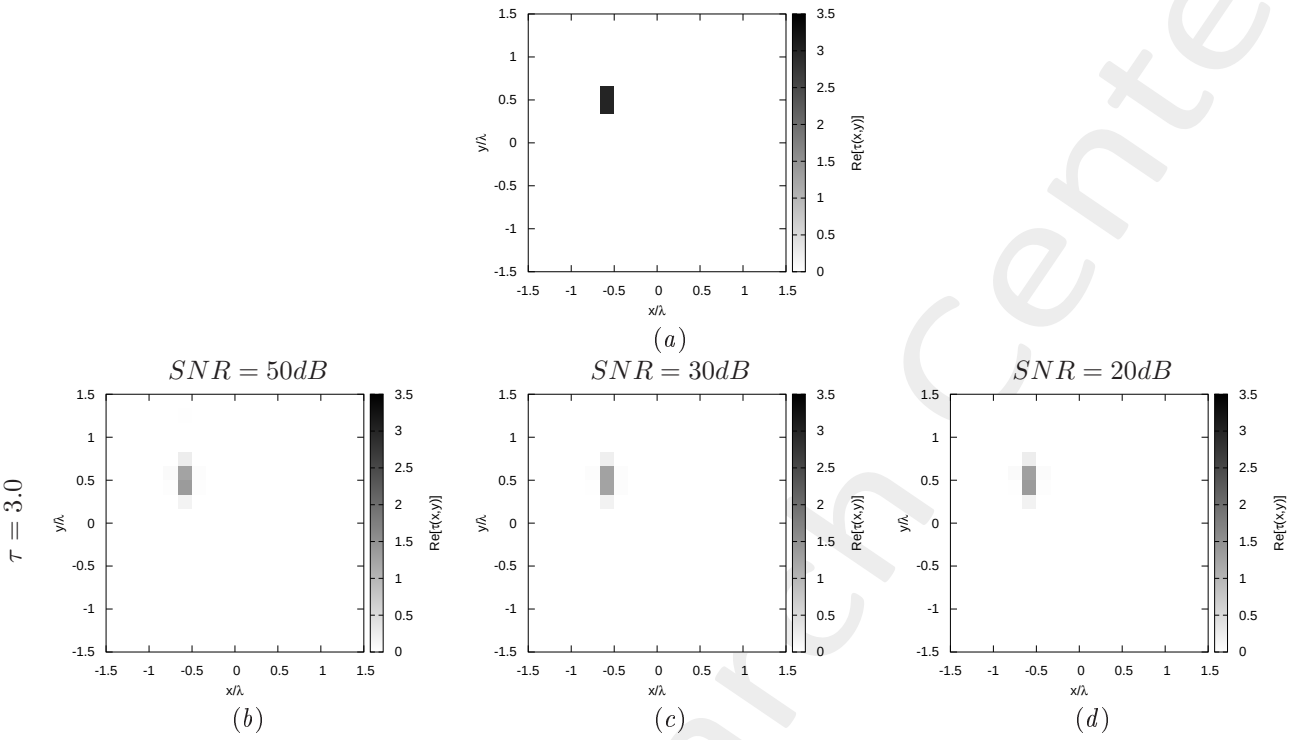

Figure 2: *Rectangle-shaped Object,* $\ell = \lambda/6$, $h = \lambda/4$: (a) Direct problem with $\tau = 3.0$, (b) ST-BCS reconstructed profiles for $SNR = 50$ [dB], (c) $SNR = 30$ [dB] and (d) $SNR = 20$ [dB]

2.1.2 Rectangle-shaped Object, $\ell = \lambda/6$, $h = \lambda/3$, - ST-BCS reconstructed profiles with Born Iterative Method ($I_{MAX} = 10$)

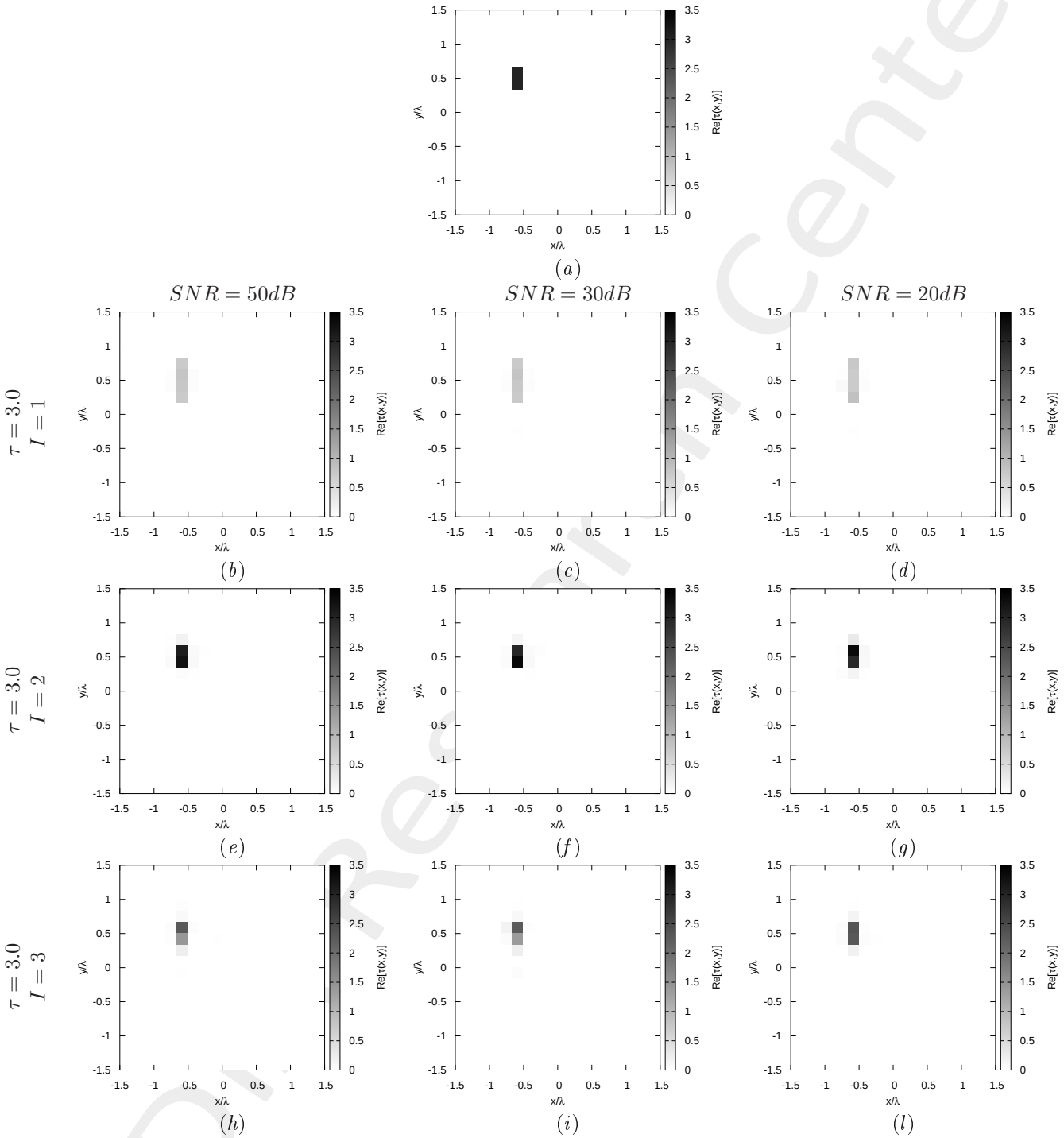

Figure 3: *Rectangle-shaped Object,* $\ell = \lambda/6$, $h = \lambda/3$: (a) Direct problem with $\tau = 3.0$, $(b)(e)(h)$ ST-BCS reconstructed profiles for $SNR = 50$ [dB], $(c)(f)(i)$ $SNR = 30$ [dB] and $(d)(g)(l)$ $SNR = 20$ [dB] with (b)-(d) Born Iterative Method at the first iteration ($I = 1$), (e)-(g) Born Iterative Method at the second iteration ($I = 2$), (h)-(l) Born Iterative Method at the third iteration ($I = 3$)

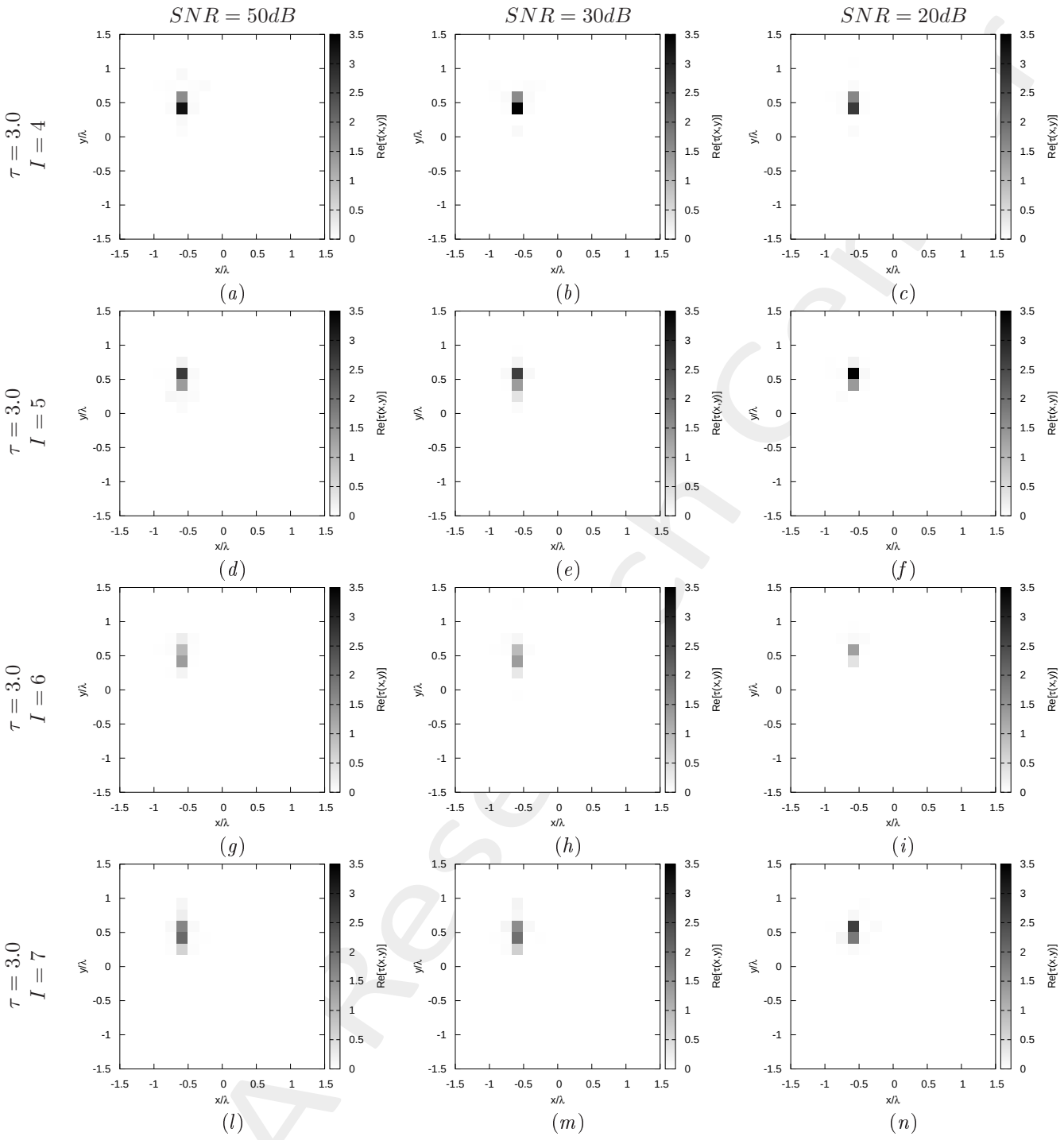

Figure 4: *Rectangle-shaped Object*, $\ell = \lambda/6$, $h = \lambda/3$: $(a)(d)(g)(l)$ ST-BCS reconstructed profiles for $SNR = 50$ [dB], $(b)(e)(h)(m)$ $SNR = 30$ [dB] and $(c)(f)(i)(n)$ $SNR = 20$ [dB] with (a)-(c) Born Iterative Method at the fourth iteration ($I = 4$), (d)-(f) Born Iterative Method at the fifth iteration ($I = 5$), (g)-(i) Born Iterative Method at the sixth iteration ($I = 6$) , (l)-(n) Born Iterative Method at the seventh iteration ($I = 7$)

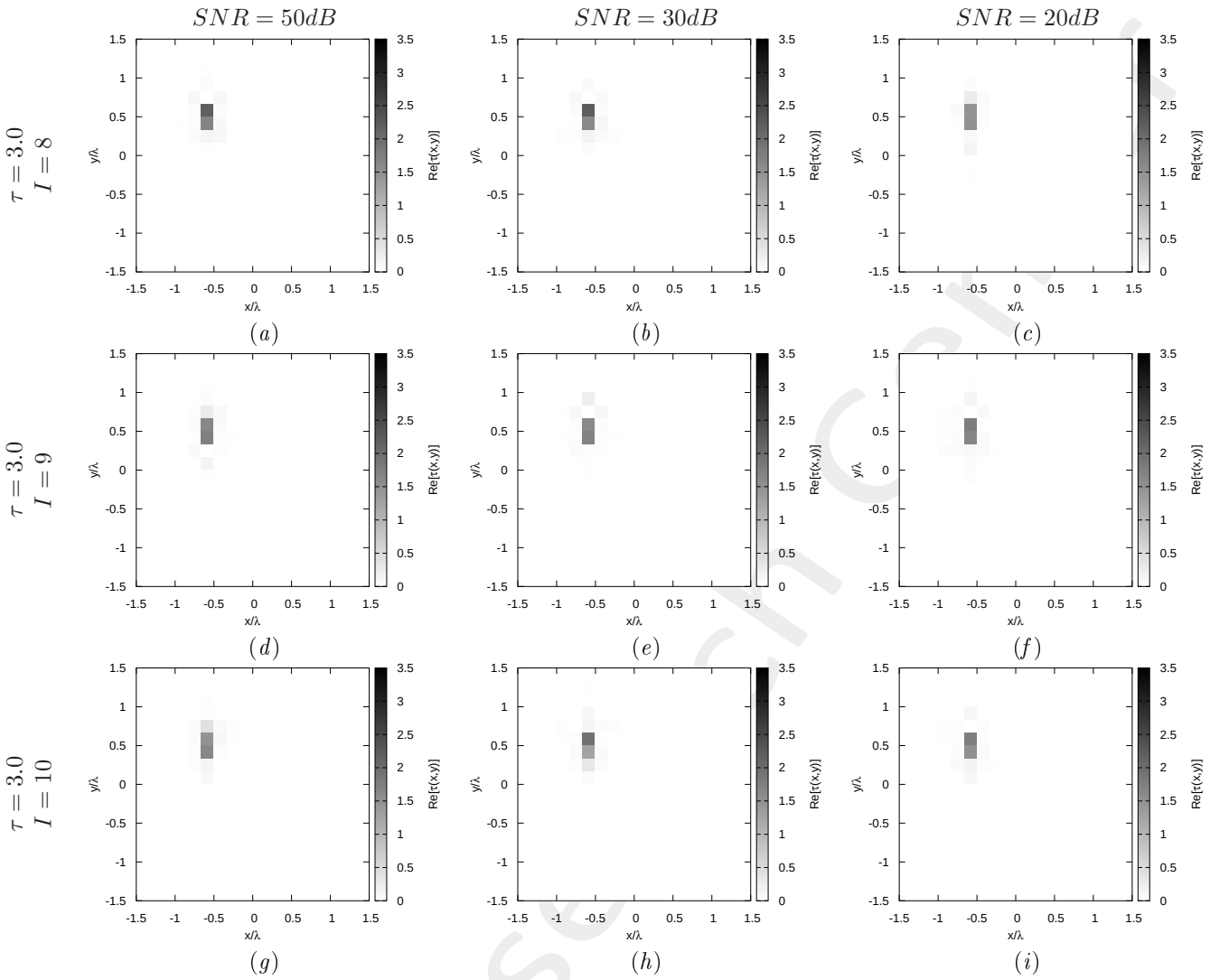

Figure 5: *Rectangle-shaped Object,* $\ell = \lambda/6$, $h = \lambda/3$: $(a)(d)(g)(l)$ ST-BCS reconstructed profiles for $SNR = 50$ [dB], $(b)(e)(h)(m)$ $SNR = 30$ [dB] and $(c)(f)(i)(n)$ $SNR = 20$ [dB] with (a)-(c) Born Iterative Method at the eighth iteration ($I = 8$), (d)-(f) Born Iterative Method at the ninth iteration ($I = 9$), (g)-(i) Born Iterative Method at the tenth iteration ($I = 10$)

2.1.3 Rectangle-shaped Object, $\ell = \lambda/6$, $h = \lambda/3$, - ST-BCS reconstructed profiles with Born Iterative Method (Threshold η)

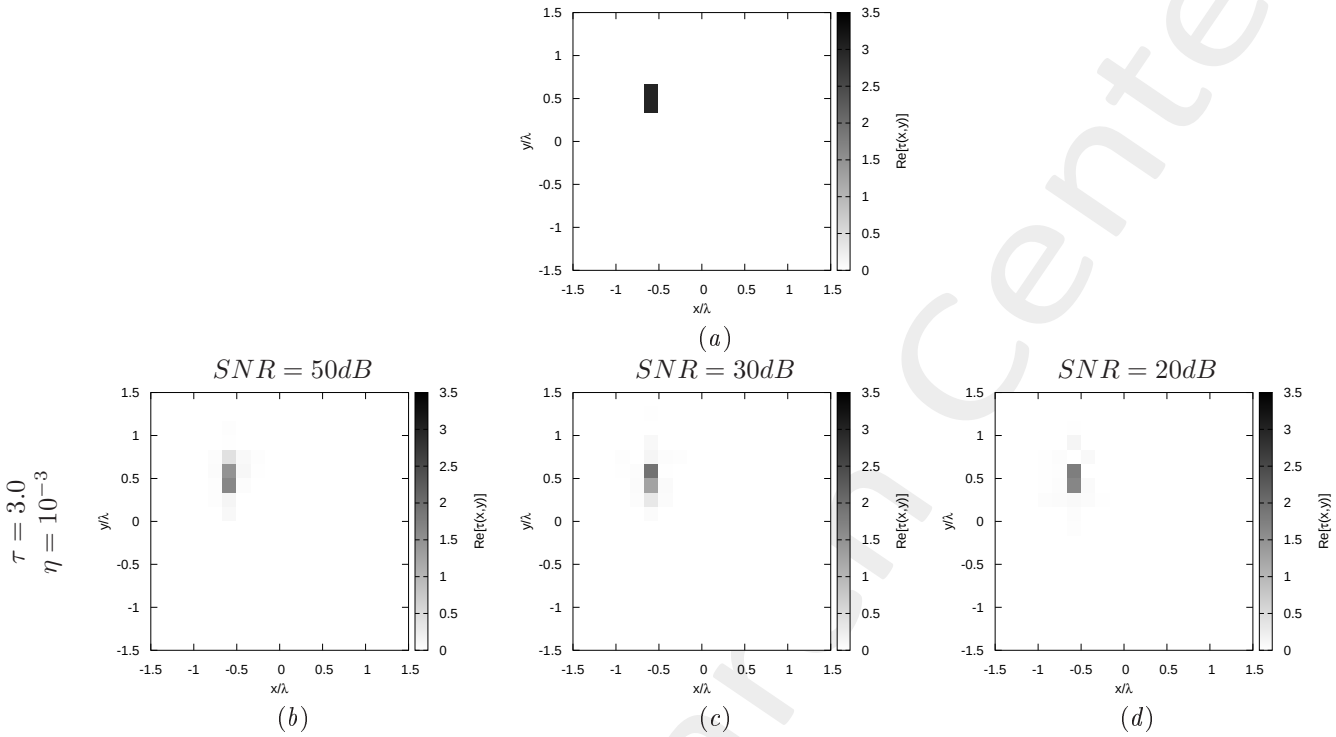

Figure 6: *Rectangle-shaped Object,* $\ell = \lambda/6$, $h = \lambda/3$: (a) Direct problem with $\tau = 3.0$, (b) ST-BCS reconstructed profiles for $SNR = 50$ [dB], (c) $SNR = 30$ [dB] and (d) $SNR = 20$ [dB] with (b)-(d) Born Iterative Method with threshold $\eta = 10^{-3}$

Tab. 1 shows the number of iterations before stopping BIM.

	$SNR = 50dB$	$SNR = 30dB$	$SNR = 20dB$
Number of iterations	10	10	9

Table I: Number of steps before the break

References

[1] G. Oliveri, M. Salucci, N. Anselmi, and A. Massa, "Compressive sensing as applied to inverse problems for imaging: theory, applications, current trends, and open challenges," *IEEE Antennas Propag. Mag.*, vol. 59, no. 5, pp. 34-46, Oct. 2017.

[2] A. Massa, P. Rocca, and G. Oliveri, "Compressive sensing in electromagnetics - A review," *IEEE Antennas Propag. Mag.*, pp. 224-238, vol. 57, no. 1, Feb. 2015.

[3] G. Oliveri, L. Poli, N. Anselmi, M. Salucci, and A. Massa, "Compressive sensing-based Born iterative method for tomographic imaging," *IEEE Trans. Microw. Theory Techn.*, vol. 67, no. 5, pp. 1753-1765, May 2019.

[4] M. Salucci, A. Gelmini, L. Poli, G. Oliveri, and A. Massa, "Progressive compressive sensing for exploiting frequency-diversity in GPR imaging," *Journal of Electromagnetic Waves and Applications*, vol. 32, no. 9, pp. 1164-1193, 2018.

[5] N. Anselmi, L. Poli, G. Oliveri, and A. Massa, "Iterative multi-resolution bayesian CS for microwave imaging," *IEEE Trans. Antennas Propag.*, vol. 66, no. 7, pp. 3665-3677, Jul. 2018.

[6] N. Anselmi, G. Oliveri, M. A. Hannan, M. Salucci, and A. Massa, "Color compressive sensing imaging of arbitrary-shaped scatterers," *IEEE Trans. Microw. Theory Techn.*, vol. 65, no. 6, pp. 1986-1999, Jun. 2017.

[7] N. Anselmi, G. Oliveri, M. Salucci, and A. Massa, "Wavelet-based compressive imaging of sparse targets," *IEEE Trans. Antennas Propag.*, vol. 63, no. 11, pp. 4889-4900, Nov. 2015.

[8] G. Oliveri, N. Anselmi, and A. Massa, "Compressive sensing imaging of non-sparse 2D scatterers by a total-variation approach within the Born approximation," *IEEE Trans. Antennas Propag.*, vol. 62, no. 10, pp. 5157-5170, Oct. 2014.

[9] L. Poli, G. Oliveri, and A. Massa, "Imaging sparse metallic cylinders through a local shape function Bayesian compressive sensing approach," *Journal of Optical Society of America A*, vol. 30, no. 6, pp. 1261-1272, 2013.

[10] L. Poli, G. Oliveri, F. Viani, and A. Massa, "MT-BCS-based microwave imaging approach through minimum-norm current expansion," *IEEE Trans. Antennas Propag.*, vol. 61, no. 9, pp. 4722-4732, Sep. 2013.

[11] L. Poli, G. Oliveri, P. Rocca, and A. Massa, "Bayesian compressive sensing approaches for the reconstruction of two-dimensional sparse scatterers under TE illumination," *IEEE Trans. Geosci. Remote Sens.*, vol. 51, no. 5, pp. 2920-2936, May 2013.

[12] L. Poli, G. Oliveri, and A. Massa, "Microwave imaging within the first-order Born approximation by means of the contrast-field Bayesian compressive sensing," *IEEE Trans. Antennas Propag.*, vol. 60, no. 6, pp. 2865-2879, Jun. 2012.

[13] G. Oliveri, L. Poli, P. Rocca, and A. Massa, "Bayesian compressive optical imaging within the Rytov approximation," *Optics Letters*, vol. 37, no. 10, pp. 1760-1762, 2012.

[14] G. Oliveri, P. Rocca, and A. Massa, "A Bayesian compressive sampling-based inversion for imaging sparse scatterers," *IEEE Trans. Geosci. Remote Sens.*, vol. 49, no. 10, pp. 3993-4006, Oct. 2011.

[15] M. Salucci, A. Gelmini, G. Oliveri, and A. Massa, "Planar arrays diagnosis by means of an advanced Bayesian compressive processing," *IEEE Trans. Antennas Propag.*, vol. 66, no. 11, pp. 5892-5906, Nov. 2018.

[16] L. Poli, G. Oliveri, P. Rocca, M. Salucci, and A. Massa, "Long-distance WPT unconventional arrays synthesis," *Journal of Electromagnetic Waves and Applications*, vol. 31, no. 14, pp. 1399-1420, Jul. 2017.

[17] G. Oliveri, M. Salucci, and A. Massa, "Synthesis of modular contiguously clustered linear arrays through a sparseness-regularized solver," *IEEE Trans. Antennas Propag.*, vol. 64, no. 10, pp. 4277-4287, Oct. 2016.

[18] P. Rocca, M. A. Hannan, M. Salucci, and A. Massa, "Single-snapshot DoA estimation in array antennas with mutual coupling through a multi-scaling BCS strategy," *IEEE Trans. Antennas Propag.*, vol. 65, no. 6, pp. 3203-3213, Jun. 2017.

[19] M. Salucci, L. Poli, and G. Oliveri, "Full-vectorial 3D microwave imaging of sparse scatterers through a multi-task Bayesian compressive sensing approach," *Journal of Imaging*, vol. 5, no. 1, pp. 1-24, Jan. 2019 (DOI: 10.3390/jimaging5010019).